Symmetry breaking and quark-hadron duality in structure functions

F. E. Close
Department of Theoretical Physics, University of Oxford, Keble Road, Oxford OX1 3NP, England

W. Melnitchouk
Jefferson Lab, 12000 Jefferson Avenue, Newport News, Virginia 23606, USA
(Received 3 February 2003; published 29 September 2003)

We identify conditions under which a summation over nucleon resonances can yield, via quark-hadron duality, parton model results for electromagnetic and neutrino structure functions at large x. While a summation over the lowest even and odd parity multiplets is sufficient to achieve duality in the symmetric quark model, a suppression of transitions to specific final states is required for more realistic cases incorporating SU(6) breaking. We outline several scenarios consistent with duality, discuss their implications for the high Q^2 behavior of transition form factors, and illustrate how they can expose the patterns in the flavor-spin dependence of interquark forces.

DOI: 10.1103/PhysRevC.68.035210 PACS number(s): 13.60.Hb, 12.40.Nn, 13.15.+g

I. INTRODUCTION

The relation between resonances and deep inelastic structure functions has been the subject of considerable interest recently. This has been partly prompted by recent high-precision data from Jefferson Lab [1] on the unpolarized F_2 structure function of the proton in the resonance region, which showed a striking similarity, when averaged over resonances, to the structure function measured at much higher energies in the deep inelastic region. This phenomenon was first observed some time ago by Bloom and Gilman [2], who found that when integrated over the mass of the inclusive hadronic final state, W, the scaling structure function at high Q^2, $F_2^{\rm scaling}$, smoothly averages that measured in the region dominated by low-lying resonances, $F_2^{\rm exp}$,

$$\int dW F_2^{\rm exp}(W^2,Q^2) = \int dW F_2^{\rm scaling}(W^2/Q^2). \qquad (1)$$

The integrand on the left-hand side of Eq. (1) represents the structure function in the resonance region at low Q^2, while that on the right-hand side corresponds to the scaling function, measured in the deep inelastic region at high Q^2. The latter is described by leading twist, perturbative QCD, as an incoherent sum over quark flavors, Σe_i^2; the former involves coherent excitation of resonances.

Global duality is said to hold after integration over all W in Eq. (1). This equality can be related to the suppression of higher twist contributions to moments of the structure function [3], in which the total moment becomes dominated by the leading twist ($\approx Q^2$ independent) component at some lower value of Q^2. Information on all coherent interaction dynamics is subsequently lost. A more local form of duality is also observed [1], in which the equality in Eq. (1) holds for restricted regions of W integration—specifically, for the three prominent resonance regions at $W \lesssim 1.8$ GeV. The duality between the resonance and scaling structure functions is also being investigated in other structure functions, such as the longitudinal structure function [4], and spin-dependent structure functions of the proton and neutron [5,6]. For spin-dependent structure functions, in particular, the workings of duality are more intricate, as the difference of cross sections no longer needs to be positive. An example is the contribution of the Δ resonance to the g_1 structure function of the proton, which is large and negative at low Q^2, but may become positive at higher Q^2.

Early work within the SU(6) symmetric quark model [7–9] showed how the ratios of various deep inelastic structure functions at $x = Q^2/2M\nu \sim 1/3$, both spin dependent and independent, could be dual to a sum over N^* resonances in the $\mathrm{SU}(6)^P = \mathbf{56}^+$ and $\mathbf{70}^-$ representations. With the emergence of precision data, showing detailed and interesting x dependence as $x \to 1$, various questions arise.

(i) How do changes in ratios as $x \to 1$ relate to the pattern of N^* resonances identified in the quark model [7–9]?
(ii) Are certain families (spin-flavor correlations) of resonances required to die out at large Q^2 in order to maintain duality? If so, can electroproduction of specific examples of such resonances test this?
(iii) Can such a program reveal the flavor-spin dependence of short distance forces in the QCD bound state?

The aim of this paper is to make a first orientation towards answering such questions. Quark models based on SU(6) spin-flavor symmetry provide benchmark descriptions of baryon spectra, as well as transitions to excited N^* states. To allow the origins of duality to remain manifest throughout our discussion, we shall restrict ourselves to the framework of the quark model, but consider the effects of SU(6) breaking explicitly. Such models serve as convenient laboratories for examining the generality of the quark-hadron duality phenomenon in more realistic scenarios than in earlier discussions. The duality between the simplest SU(6) quark-parton model results [10] for ratios of structure functions with sums over the $\mathbf{56}^+$ and $\mathbf{70}^-$ coherent N^* excitations was described in Refs. [7,8,11]. An essential feature of those analyses was that SU(6) was exact and that exotics in the t-channel were suppressed. In a global sense such results are self-consistent: the absence of t-channel exotics equates with an absence of $\gamma\gamma \to q\bar{q}q\bar{q}$ couplings, and hence, in effect, to

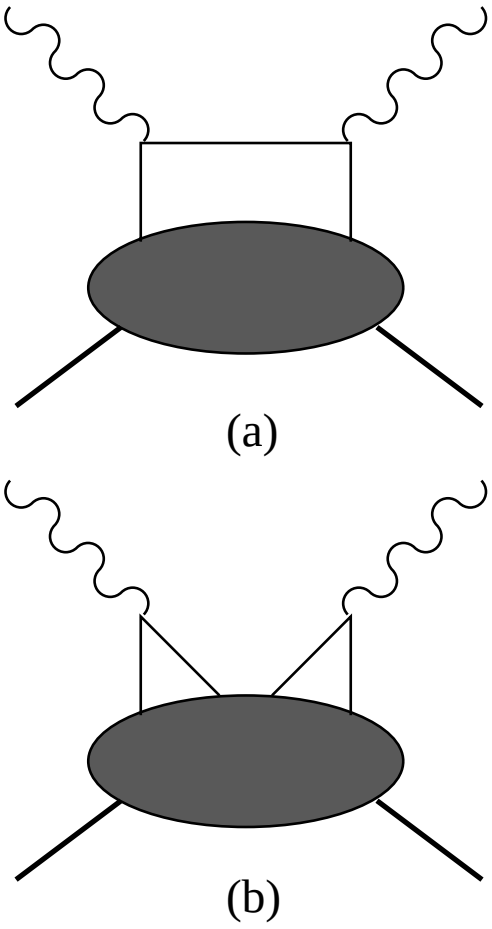

FIG. 1. (a) Leading twist structure function, with photons coupling to the same quark; (b) higher twist contributions involving coupling to different quarks in the nucleon.

the presence only of incoherent diagrams where the photons couple to the same quark, $\gamma q \to \gamma q$ [see Fig. 1(a)].

Although the *s*-channel sum was shown to be dual for ratios of incoherent quantities [7–9], this alone did not explain why (or if) any individual sum over states scaled. Recently, the transition from resonances to scaling has been explored in microscopic models at the quark level. The phenomenological quark model duality of Refs. [7–9] was recently shown [12] to arise in a simple model of spinless constituents. A model in which the hadron consisted of a pointlike scalar ''quark'' bound to an infinitely massive core by a harmonic oscillator potential was used [13] to explicitly demonstrate how a sum over infinitely narrow resonances can lead to a structure function which scales in the $Q^2 \to \infty$ limit. These ideas have been further developed [14] to give an increasingly solid model underpinning of this phenomenological duality.

Since the original quark model predictions were made in the 1970s, the quantity and quality of structure function data have improved dramatically. We now know, for instance, that in some regions of x SU(6) symmetry is badly broken, with the strongest deviations from the naive SU(6) expectations being prevalent at large values of x. The new data will set challenges for theories of quark-hadron duality. There are critical questions which now need to be addressed.

(i) Can duality survive locally in x, and what do the observed variations in x require of N^* excitations if duality is to survive?
(ii) What families [spin-flavor correlations, or SU(6) multiplets] are suppressed as $x \to 1$, or equivalently $Q^2 \to \infty$, for duality to hold?
(iii) Does the excitation of low-lying prominent N^* resonances, belonging to such families, exhibit such behavior?

If the $x \to 1$ systematics for N^* families are not matched by specific $N \to N^*$ transition form factors as a function of Q^2, then duality fails. If, however, they do match, then this can expose the patterns in the flavor-spin dependence of interquark forces.

In this paper we explore the question of whether quark-hadron duality exists in structure functions for the more realistic scenario in which SU(6) is explicitly broken. We focus on both electromagnetic and neutrino scattering. While most of the phenomenological information comes from electron scattering, neutrino-induced reactions provide an important consistency check on the derived duality relations, and predictions for neutrino structure function ratios can be tested once high-intensity neutrino beams become available [15]. After reviewing the symmetric SU(6) quark model results for structure functions in Sec. II, we identify in Sec. III the necessary patterns of $N \to N^*$ suppression in order to obtain structure functions which are compatible with data and expectations from hard scattering at large x and higher Q^2. In the process we derive duality relations for various structure function ratios, in which the breaking of SU(6) symmetry is parametrized in terms of x-dependent mixing angles. Fixing the mixing angles by the unpolarized neutron to proton structure function ratio data then allows us to make explicit predictions for the x dependence of polarization asymmetries for the proton and neutron, under various symmetry breaking scenarios. Experimental signatures for the corresponding $N \to N^*$ suppressions are discussed in Sec. IV, and conclusions and ideas for future developments summarized in Sec. V.

II. DUALITY AND THE QUARK MODEL

The SU(6) spin-flavor symmetric quark model serves as a useful basis in which one may visualize both the principles underpinning the phenomenon of quark-hadron duality and at the same time provide a reasonably close contact with phenomenology. Following earlier work in Refs. [7–9,11,16], it was shown by Close and Isgur [12] that the structure function ratios of the symmetric quark model can be obtained by summing over appropriate sets of baryon resonances. Higher twist effects, which give rise to violations of duality through nondiagonal quark transitions, such as in the ''cat's ears'' diagram in Fig. 1(b), can be shown to cancel in a small energy range appropriate for summing over neighboring odd and even parity states. In the SU(6) quark model this corresponds to summing over states in the $\mathbf{56}^+$ $(L=0)$ and $\mathbf{70}^-$ $(L=1)$ multiplets, with each representation weighted equally. The spin-averaged transverse F_1 structure function, for instance, in this framework is given by the sum

TABLE I. Relative strengths of electromagnetic $N \to N^*$ transitions in the SU(6) quark model. The coefficients λ and ρ denote the relative strengths of the symmetric and antisymmetric contributions of the SU(6) ground state wave function. The SU(6) limit corresponds to $\lambda = \rho$.

SU(6) representation	$^2\mathbf{8}[\mathbf{56}^+]$	$^4\mathbf{10}[\mathbf{56}^+]$	$^2\mathbf{8}[\mathbf{70}^-]$	$^4\mathbf{8}[\mathbf{70}^-]$	$^2\mathbf{10}[\mathbf{70}^-]$	Total
F_1^p	$9\rho^2$	$8\lambda^2$	$9\rho^2$	0	λ^2	$18\rho^2+9\lambda^2$
F_1^n	$(3\rho+\lambda)^2/4$	$8\lambda^2$	$(3\rho-\lambda)^2/4$	$4\lambda^2$	λ^2	$(9\rho^2+27\lambda^2)/2$
g_1^p	$9\rho^2$	$-4\lambda^2$	$9\rho^2$	0	λ^2	$18\rho^2-3\lambda^2$
g_1^n	$(3\rho+\lambda)^2/4$	$-4\lambda^2$	$(3\rho-\lambda)^2/4$	$-2\lambda^2$	λ^2	$(9\rho^2-9\lambda^2)/2$

of squares of form factors, $F_{N\to R}(\vec{q}^2)$, describing the transitions from the nucleon to excited states R,

$$F_1(\nu,\vec{q}^2) \sim \sum_R |F_{N\to R}(\vec{q}^2)|^2 \delta(E_R - E_N - \nu), \tag{2}$$

where E_N and E_R are the energies of the ground state and excited state, respectively. In terms of photoabsorption cross sections (or W boson absorption cross sections for neutrino scattering), the F_1 structure function is proportional to the sum $\sigma_{1/2}+\sigma_{3/2}$, with $\sigma_{1/2(3/2)}$ the cross section for total boson-nucleon helicity 1/2 (3/2). The spin-dependent g_1 structure function, on the other hand, corresponds to the difference $\sigma_{1/2}-\sigma_{3/2}$.

Resonance excitation and deep inelastic scattering in general involve both electric and magnetic multipoles. Excitation in a given partial wave at $Q^2=0$ involves a complicated mix of these. However, as Q^2 grows one expects the magnetic multipole to dominate over the electric, even by $Q^2 \sim 0.5\ \mathrm{GeV}^2$ in specific models [7,11]. Furthermore, recent phenomenological analyses of electromagnetic excitations of negative parity resonances suggest that for the prominent D_{13} resonance the ratio of helicity-1/2 to helicity-3/2 amplitudes is consistent with zero beyond $Q^2 \approx 2\ \mathrm{GeV}^2$ [17], which corresponds to magnetic dominance. This dominance of magnetic, or spin flip, interactions at large Q^2 for N^* excitation matches the dominance of such spin flip in deep inelastic scattering. For instance, the polarization asymmetry $A_1 = g_1/F_1$ is positive at large Q^2, whereas $A_1 < 0$ if electric interactions were prominent [18]. Thus in the present analysis we assume that the interaction with the quark is dominated by the magnetic coupling. In this approximation the F_1 and F_2 structure functions are simply related by the Callan-Gross relation, $F_2 = 2xF_1$, independent of the specific models we use for the structure functions themselves.

The relative photoproduction strengths of the transitions from the ground state to the $\mathbf{56}^+$ and $\mathbf{70}^-$ are summarized in Table I for the F_1 and g_1 structure functions of the proton and neutron. For generality, we separate the contributions from the symmetric and antisymmetric components of the ground state nucleon wave function, with strengths λ and ρ, respectively. The SU(6) limit corresponds to $\lambda = \rho$. The coefficients in Table I assume equal weights for the $\mathbf{56}^+$ and $\mathbf{70}^-$ multiplets [7]. Similarly, neutrino-induced transitions to excited states can be evaluated [8], and the relative strengths are displayed in Table II for the proton and neutron. Because of charge conservation, only transitions to decuplet (isospin-$\frac{3}{2}$) states from the proton are allowed. (Note that the overall normalizations of the electromagnetic and neutrino matrix elements in Tables I and II are arbitrary.)

Summing over the full set of states in the $\mathbf{56}^+$ and $\mathbf{70}^-$ multiplets leads to definite predictions for neutron and proton structure function ratios,

$$R^{np} = \frac{F_1^n}{F_1^p}, \tag{3}$$

$$R^{\nu} = \frac{F_1^{\nu p}}{F_1^{\nu n}}, \tag{4}$$

and polarization asymmetries,

$$A_1^N = \frac{g_1^N}{F_1^N}, \tag{5}$$

$$A_1^{\nu N} = \frac{g_1^{\nu N}}{F_1^{\nu N}}, \tag{6}$$

for $N = p$ or n. In particular, for $\lambda = \rho$ one finds the classic SU(6) quark-parton model results [19]:

$$R^{np} = \frac{2}{3}, \quad A_1^p = \frac{5}{9}, \quad A_1^n = 0 \quad [\mathrm{SU}(6)], \tag{7}$$

for electromagnetic scattering, and

TABLE II. As in Table I, but for neutrino-induced $N \to N^*$ transitions.

SU(6) representation	$^2\mathbf{8}[\mathbf{56}^+]$	$^4\mathbf{10}[\mathbf{56}^+]$	$^2\mathbf{8}[\mathbf{70}^-]$	$^4\mathbf{8}[\mathbf{70}^-]$	$^2\mathbf{10}[\mathbf{70}^-]$	Total
$F_1^{\nu p}$	0	$24\lambda^2$	0	0	$3\lambda^2$	$27\lambda^2$
$F_1^{\nu n}$	$(9\rho+\lambda)^2/4$	$8\lambda^2$	$(9\rho-\lambda)^2/4$	$4\lambda^2$	λ^2	$(81\rho^2+27\lambda^2)/2$
$g_1^{\nu p}$	0	$-12\lambda^2$	0	0	$3\lambda^2$	$-9\lambda^2$
$g_1^{\nu n}$	$(9\rho+\lambda)^2/4$	$-4\lambda^2$	$(9\rho-\lambda)^2/4$	$-2\lambda^2$	λ^2	$(81\rho^2-9\lambda^2)/2$

TABLE III. Structure function ratios from quark-hadron duality in SU(6), and in various SU(6) breaking scenarios, as described in the text. Note that the "No ^{4}**10**" and "No ^{2,4}**10**" scenarios are not consistent with quark-hadron duality.

Model	SU(6)	No ^{4}**10**	No ^{2}**10**, ^{4}**10**	No $S_{3/2}$	No $\sigma_{3/2}$	No ψ_λ
R^{np}	2/3	10/19	1/2	6/19	3/7	1/4
A_1^p	5/9	1	1	1	1	1
A_1^n	0	2/5	1/3	1	1	1
R^ν	1/2	3/46	0	1/14	1/5	0
$A_1^{\nu p}$	−1/3	1		1		−1/3
$A_1^{\nu n}$	2/3	20/23	13/15	1	1	1

$$R^\nu=\frac{1}{2},\quad A_1^{\nu p}=-\frac{1}{3},\quad A_1^{\nu n}=\frac{2}{3}\quad [\mathrm{SU}(6)], \tag{8}$$

for neutrino scattering, which correspond to $u=2d$ and $\Delta u=-4\Delta d$. The quark level results are easily deduced by considering the wave function of a proton in the SU(6) limit, polarized in the $+z$ direction [19]:

$$|p^\uparrow\rangle=\frac{1}{\sqrt{2}}|u^\uparrow(ud)_0\rangle+\frac{1}{\sqrt{18}}|u^\uparrow(ud)_1\rangle-\frac{1}{3}|u^\downarrow(ud)_1\rangle$$
$$-\frac{1}{3}|d^\uparrow(uu)_1\rangle-\frac{\sqrt{2}}{3}|d^\downarrow(uu)_1\rangle, \tag{9}$$

where the subscript 0 or 1 denotes the total spin of the two-quark component. The neutron wave function is obtained from Eq. (9) by interchanging $u\leftrightarrow d$. In this limit, apart from charge and flavor quantum numbers, the u and d quarks in the proton are identical, and, in particular, have the same x distributions. The relations between the structure functions and leading order parton distributions are given in the Appendix. The various structure function ratios in the SU(6) quark model are listed in the first column of Table III.

One should point out that these results arise in an ideal world of SU(6) symmetry where the members of a $\mathbf{56}^+$ or $\mathbf{70}^-$ are each degenerate, with common Q^2 dependent form factors. Reality is not like that. In the quark model the usual assignments of the excited states have the nucleon and $P_{33}(1232)$ Δ isobar belonging to the quark spin-$\frac{1}{2}$ ^{2}**8** and quark spin-$\frac{3}{2}$ ^{4}**10** representations of $\mathbf{56}^+$, respectively, while for the odd parity states the ^{2}**8** representation contains the states $S_{11}(1535)$ and $D_{13}(1520)$, the ^{4}**8** contains the $S_{11}(1650)$, $D_{13}(1700)$, and $D_{15}(1675)$, while the isospin-$\frac{3}{2}$ states $S_{31}(1620)$ and $D_{33}(1700)$ belong to the ^{2}**10** representation. One purpose of this paper will be to investigate the systematics of such SU(6) breaking which split energy levels, give different Q^2 dependence to form factors, distort the u and d flavors and spin distributions, and affect the $x\to1$ behaviors via duality.

III. DUALITY AND SU(6) BREAKING

While the SU(6) predictions for the structure functions hold approximately at $x\sim1/3$, significant deviations are observed at larger x. Empirically, the d quark distribution is observed to be much softer than the u for $x\gtrsim0.5$ [19–22], leading to $F_2^n/F_2^p\ll2/3$ at large x. Also, on the basis of helicity conservation [23,24], one expects that the proton and neutron polarization asymmetries, for both electromagnetic and neutrino scattering, $A_1^N, A_1^{\nu N}\to1$ as $x\to1$, in dramatic contrast to the SU(6) expectations, especially for the neutron, where $A_1^n=0$ and $A_1^{\nu n}=-1/3$.

In this section we examine the conditions under which combinations of resonances can reproduce, via quark-hadron duality, the behavior of structure functions in the large-x region where SU(6) breaking effects are most prominent. At the quark level, explicit SU(6) breaking mechanisms produce different weightings of components of the initial state wave function, Eq. (9), which in turn induces different x dependences for the spin and flavor distributions. On the other hand, at the hadronic level SU(6) breaking in the $N\to N^*$ matrix elements leads to suppression of transitions to specific resonances in the final state, while starting from a symmetric SU(6) initial state wave function. Thus if we admit breaking of the SU(6) symmetry, then for duality to be manifest the pattern of symmetry breaking in the initial state has to match that in the final state.

Note that for a fixed $W=M_R$ of a given resonance R, the resonance peak moves to larger x with increasing Q^2, since at the resonance peak one has $x=x_R\equiv Q^2/(M_R^2-M^2+Q^2)$. At low Q^2, the prominent resonances are spread out in x and a necessary condition for duality involves integrating over a range of x corresponding to $W\lesssim2$ GeV. At large Q^2 for fixed x one has large W and hence a dense population of overlapping coherent resonance states. In such a circumstance duality can become locally satisfied. In turn this kinematics means that if a given resonance at $x\sim1/3$ appears at relatively low Q^2, the $x\sim1$ behavior of the resonance contribution to the structure function will be determined by the $N\to R$ transition form factor at large Q^2.

We shall look therefore for different Q^2 dependences in the transition form factors to different spin-flavor multiplets, and study their implications for $x\to1$ in the sum. Then we shall look at specific examples of resonances having these particular correlations and identify experimental tests of the hypothesis.

A. Suppression of Δ states

The most immediate breaking of the SU(6) duality could be achieved by varying the overall strengths of the coeffi-

cients for the $\mathbf{56}^+$ and $\mathbf{70}^-$ multiplets as a whole. However, since the cancellations of the $N \to N^*$ transitions for the case of g_1^n occur within each multiplet, a nonzero value of A_1^n can only be achieved if SU(6) is broken *within* each multiplet rather than *between* the multiplets. Some intuition is needed therefore on sensible breaking patterns within the supermultiplets.

Turning first to the $\mathbf{56}^+$, empirical evidence suggests that at high Q^2 the $N \to \Delta$ transition form factor is anomalously suppressed relative to the elastic nucleon form factors [25,26]. This phenomenon has been attributed to spin-dependent forces between quarks, such as from single gluon exchange [27], which split the nucleon and Δ masses and necessarily break SU(6). Removing the $^4\mathbf{10}[\mathbf{56}^+]$ from the s-channel sum causes R^{np} to fall (to $10/19 \approx 0.53$), as required phenomenologically, and both A_1^p and A_1^n to increase (to 1 and 2/5, respectively) compared with the SU(6) values (see column 2 of Table III).

Investigation of the coefficients in Tables I and II, however, shows that a suppression of the Δ alone is not consistent with quark-hadron duality. In particular, it gives rise to a $\Delta u/u$ ratio, extracted from the electromagnetic structure functions [see Eq. (A6) in the Appendix], which is greater than unity, thereby violating a partonic interpretation of the structure functions. Similarly, suppression of all decuplet contributions, namely the $^4\mathbf{10}$ in the $\mathbf{56}^+$ and $^2\mathbf{10}$ in the $\mathbf{70}^-$ (column 3 of Table III), still gives a value for the extracted $\Delta u/u$ which exceeds unity.

The reason for the failure of duality here is that eliminating Δ states in the s-channel sum spoils the cancellation of exotic exchanges in the t channel, $\gamma\gamma \to N\bar{N}$. Nonexotic **1** and **35** SU(6) representations correspond to $q\bar{q}$, thus in the t channel these appear as $\gamma\gamma \to q\bar{q}$; when such a diagram is viewed in the s channel one sees that in effect it can map onto handbag or leading twist topologies, enabling a partonic interpretation, as shown in Fig. 1(a). Exotic exchanges, such as **405**, require $qqq\bar{q}$ in the t channel, and map onto higher twist contributions, such as in Fig. 1(b). These are incompatible with single parton probability interpretations in principle, with the specific $\Delta u/u > 1$ result illustrating this.

Moreover, the results for the $\Delta u/u$ and $\Delta d/d$ ratios extracted from the electromagnetic observables, namely $\Delta u/u = 23/21$ and $\Delta d/d = -1/3$, do not agree with those obtained from the neutrino polarization asymmetries $A_1^{\nu N}$ (column 3 of Table III). In addition, for both of these scenarios the ratio d/u extracted from R^{np} does not match that obtained from R^{ν}. These are all consequences of the presence of t-channel exotics in such scenarios, and further underscore the inconsistency of duality with suppression of Δ states alone.

B. Spin $\frac{3}{2}$ suppression

If the characteristic Q^2 dependence for Δ excitation is indeed due to spin dependence, then it may be that this is a phenomenon realized by all $S = 3/2$ quark couplings, namely $^4\mathbf{10}[\mathbf{56}^+]$ and $^4\mathbf{8}[\mathbf{70}^-]$. An immediate observation in this scenario from Tables I and II is that each of the contributions corresponding to (the surviving) quark spin $S = 1/2$ configurations has equal strength for g_1 and F_1, which automatically gives unity for the polarization asymmetries A_1. This simply follows from the (high Q^2) approximation that only magnetic couplings to quarks contribute, so that only $S = 3/2$ configurations allow nonzero $\sigma_{3/2}$ cross sections (we shall return to this later).

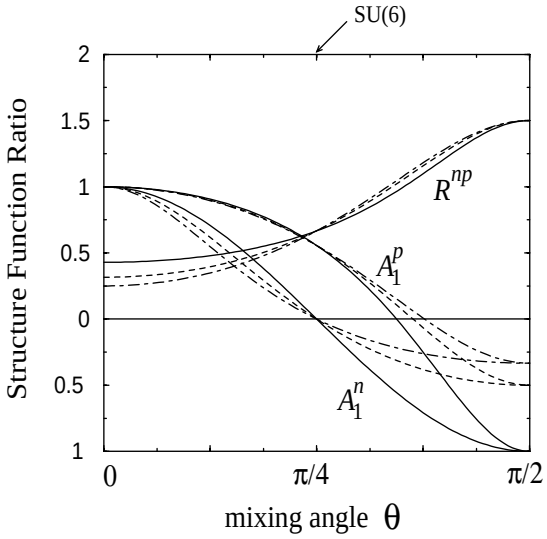

FIG. 2. Electromagnetic structure function ratios for different combinations of $\sigma_{1/2}$ and $\sigma_{3/2}$ cross sections ($\theta = \theta_s$, solid), quark spins $S_{1/2}$ and $S_{3/2}$ ($\theta = \theta_h$, dashed), and the symmetric "λ" and antisymmetric "ρ" components of the ground state wave function ($\theta = \theta_w$, dot-dashed). The SU(6) corresponds to $\theta = \pi/4$.

More generally, one can observe that duality is satisfied by summing over the individual $S = 1/2$ and $S = 3/2$ contributions separately, $S_{1/2} \equiv {}^2\mathbf{8}[\mathbf{56}^+] + {}^2\mathbf{8}[\mathbf{70}^-] + {}^2\mathbf{8}[\mathbf{70}^-]$, and $S_{3/2} \equiv {}^4\mathbf{10}[\mathbf{56}^+] + {}^4\mathbf{8}[\mathbf{70}^-]$. If the relative contributions of the $S_{1/2}$ and $S_{3/2}$ channels are weighted by $\cos^2\theta_s$ and $\sin^2\theta_s$, respectively, then the ratio of unpolarized neutron to proton structure functions can be written as

$$R^{np} = \frac{6(1+\sin^2\theta_s)}{19 - 11\sin^2\theta_s}, \tag{10}$$

and the polarization asymmetries become

$$A_1^p = \frac{19 - 23\sin^2\theta_s}{19 - 11\sin^2\theta_s}, \tag{11}$$

$$A_1^n = \frac{1 - 2\sin^2\theta_s}{1 + \sin^2\theta_s}. \tag{12}$$

The dependence on the mixing angle θ_s of these ratios is illustrated in Fig. 2 (dashed curves). The SU(6) symmetric limit, Eq. (7), is reproduced when $\theta_s = \pi/4$, as indicated in Fig. 2. As $\theta_s \to 0$, corresponding to $S_{1/2}$ dominance, the neutron to proton ratio decreases, and both the polarization asymmetries approach their maximal values,

$$R^{np} = \frac{6}{19}, \quad A_1^p = 1, \quad A_1^n = 1 \quad [\theta_s = 0]. \tag{13}$$

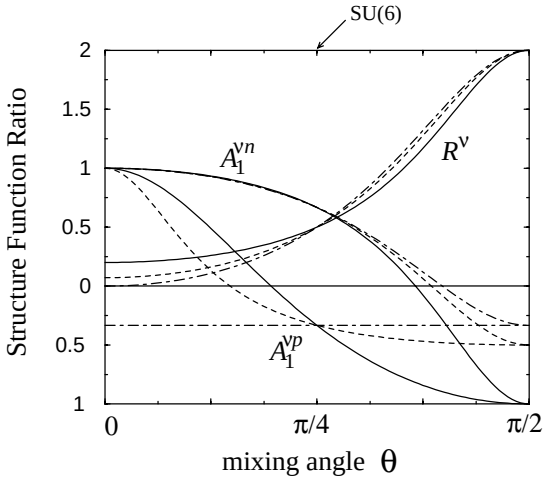

FIG. 3. As in Fig. 2, but for neutrino scattering ratios.

In the other extreme limit as $\theta_s \to \pi/2$, the polarization asymmetries approach -1, while $R^{np} \to 3/2$. Neither of these scenarios are supported phenomenologically, as we shall discuss below, and the physical region appears to correspond to $0 \lesssim \theta_s \lesssim 9\pi/32$.

In analogy with Eqs. (10)–(12), the ratio of the unpolarized proton and neutron structure functions for neutrino scattering is

$$R^{\nu} = \frac{1 + 7\sin^2\theta_s}{14 - 10\sin^2\theta_s}, \tag{14}$$

and the neutrino polarization asymmetries:

$$A_1^{\nu p} = \frac{1 - 5\sin^2\theta_s}{1 + 7\sin^2\theta_s}, \tag{15}$$

$$A_1^{\nu p} = \frac{7 - 8\sin^2\theta_s}{7 - 5\sin^2\theta_s}. \tag{16}$$

The dependence on the angle θ_s for the neutrino observables is shown in Fig. 3 (dashed curves). The trends of the ratios are similar to those of the electromagnetic ratios in Fig. 2 (with the neutron and proton reversed). Once again the SU(6) symmetric limit, Eq. (8), is reproduced when $\theta_s = \pi/4$. The phenomenologically favored scenario in which $S_{3/2}$ contributions are suppressed in the limit $x \to 1$ gives rise to

$$R^{\nu} = \frac{1}{14}, \quad A_1^{\nu p} = 1, \quad A_1^{\nu n} = 1 \quad [\theta_s = 0]. \tag{17}$$

From the relations between the structure functions and parton distributions in the Appendix one can verify that the results for d/u extracted from R^{np} are consistent with those from R^{ν} [Eqs. (A5) and (A12)], and those for $\Delta q/q$ extracted from A_1^N consistent with those from $A_1^{\nu N}$ [Eqs. (A6)–(A7) and Eqs. (A13)–(A14)].

The dependence of the structure function ratios in Eqs. (10)–(12) and Eqs. (14)–(16) on one parameter θ_s means

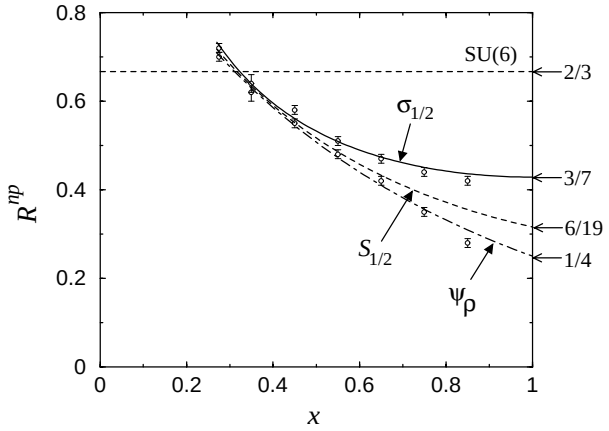

FIG. 4. Ratio R^{np} of unpolarized neutron to proton structure functions from duality, according to different scenarios of SU(6) breaking: helicity $\sigma_{1/2}$ dominance (solid); spin $S_{1/2}$ dominance (dashed); ψ_ρ dominance (dot-dashed). Various theoretical predictions for the $x \to 1$ limit are indicated on the ordinate. The data are from SLAC [20,21], analyzed under different assumptions (see text) about the size of the nuclear EMC effects in the deuteron [22].

that the SU(6) breaking scenario with $S_{3/2}$ suppression can be tested by simultaneously fitting the n/p ratios and the polarization asymmetries. In general, data on unpolarized structure functions are more abundant, especially at high x, than on spin-dependent structure functions, so it is more practical to fit the x dependence of $\theta_s(x)$ to the existing data on unpolarized n/p ratios, which can then be used to predict the polarization asymmetries.

Unfortunately, data on F_1 neutrino structure functions at $x \gtrsim 0.4$–0.5 are essentially nonexistent, and there have been no experiments at all to measure spin-dependent structure functions in neutrino scattering. The most precise data on the electromagnetic neutron to proton ratio R^{np} come from SLAC experiments [20,21]. The absence of free neutron targets has meant that neutron structure information has had to be inferred from inclusive deuteron and proton structure functions. Because of uncertainties in the treatment of

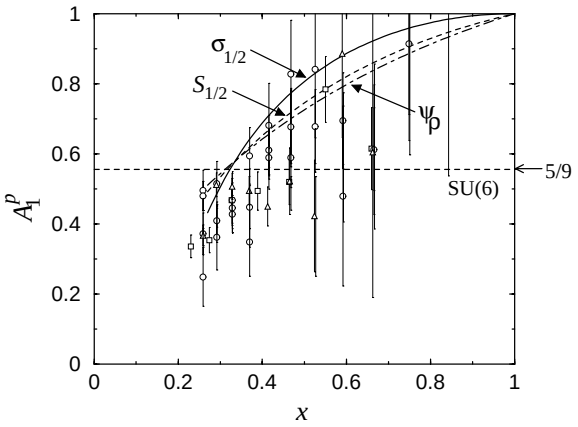

FIG. 5. As in Fig. 4, but for the proton polarization asymmetry A_1^p. The data are a compilation (for $x \gtrsim 0.2$) from experiments at SLAC [32], from the SMC [33], and HERMES Collaborations [34].

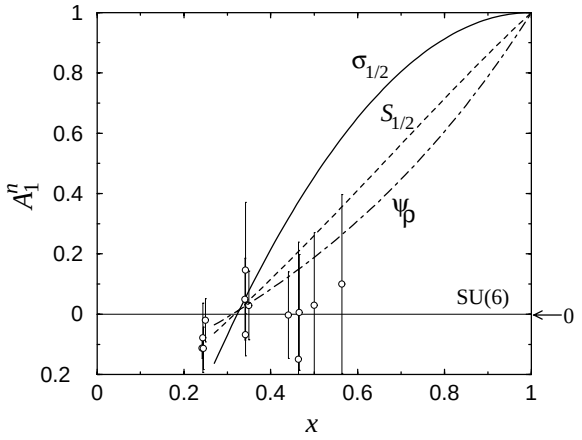

FIG. 6. As in Fig. 5, but for the neutron polarization asymmetry A_1^n.

nuclear corrections in the deuteron at large x, however, which is more sensitive to the high momentum components of the deuteron wave function, the results beyond $x \sim 0.6$ are somewhat model dependent [22], as indicated in Fig. 4. The difference between the two sets of points is representative of the theoretical uncertainty in the extraction. In particular, the lower set of points corresponds to an analysis which accounts for Fermi motion in the deuteron [28], while the upper set of points includes Fermi motion and binding effects [22] (see also Ref. [29]). A fit to the weighted average of the extrema of the two sets of data points, constrained to approach $R^{np}=6/19$ as $x \to 1$, is indicated by the dashed curve [a polynomial of degree two is used to fit the x dependence of $\theta_s(x)$ in Eq. (10)]. The fit is clearly compatible with the current data on R^{np}, but could be further constrained by more accurate data at large x. Several proposals for obtaining the neutron to proton ratio at large x with reduced nuclear uncertainties are discussed in Refs. [30,31].

Using the mixing angle $\theta_s(x)$ fitted to R^{np}, the resulting polarization asymmetries for the proton and neutron are shown in Figs. 5 and 6, respectively, compared with a compilation of large-x data from SLAC [32], SMC [33], and

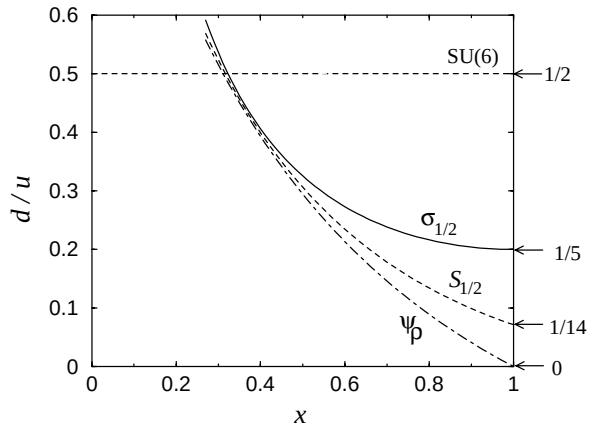

FIG. 7. Unpolarized d/u $(=R^\nu)$ ratio in various SU(6) breaking scenarios, as described in the text.

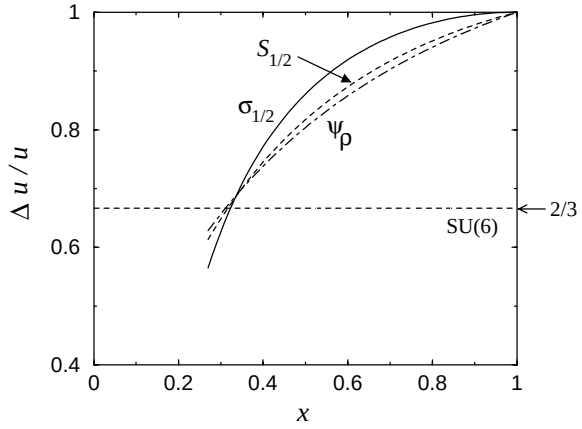

FIG. 8. Ratio of polarized to unpolarized u quark distributions, $\Delta u/u$ $(=A_1^{\nu n})$, in various SU(6) breaking scenarios.

HERMES [34]. The predicted x dependence of both A_1^p and A_1^n in the $S_{3/2}$ suppression scenario is relatively strong; the SU(6) symmetric results which describe the data at $x \sim 1/3$ rapidly give way to the broken SU(6) predictions as $x \to 1$. Within the current experimental errors, the $S_{3/2}$ suppression model is consistent with the x dependence of both the R^{np} ratio and the polarization asymmetries.

Using the neutrino ratios R^ν, $A_1^{\nu p}$, and $A_1^{\nu n}$, the individual quark flavor and spin distribution ratios can be determined (or equivalently, extracted from the electromagnetic ratios as discussed in the Appendix). The unpolarized d/u ratio in the $S_{1/2}$ dominance scenario is shown in Fig. 7 (dashed), and the spin-flavor ratios $\Delta u/u$ and $\Delta d/d$ are illustrated in Figs. 8 and 9, respectively.

C. Helicity 3/2 suppression

The above discussion has demonstrated how duality between the parton model and a sum over low-lying resonances can arise on the basis of classifying transitions to excited states according to the total spin of the quarks, with either equal weighting of $S_{1/2}$ and $S_{3/2}$ components in the case of SU(6) symmetry, or suppression of the latter at large x. According to duality, structure functions at large x are determined by the behavior of transition form factors at high Q^2;

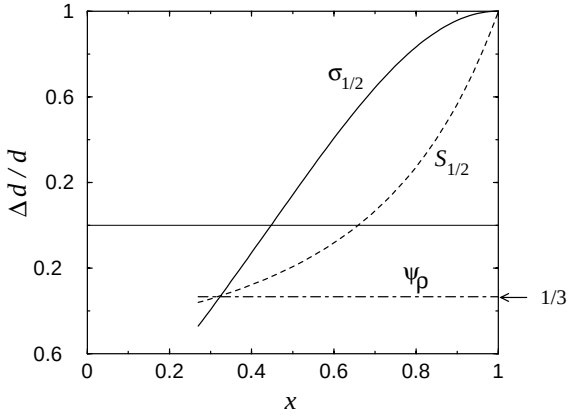

FIG. 9. As in Fig. 8, but for the $\Delta d/d$ $(=A_1^{\nu p})$ ratio.

TABLE IV. Relative strengths of electromagnetic $N \to N^*$ transitions corresponding to $\sigma_{1/2}$ dominance. These values can be obtained from Table I by adding the F_1 and g_1 contributions.

SU(6) representation	$^2\mathbf{8}[\mathbf{56}^+]$	$^4\mathbf{10}[\mathbf{56}^+]$	$^2\mathbf{8}[\mathbf{70}^-]$	$^4\mathbf{8}[\mathbf{70}^-]$	$^2\mathbf{10}[\mathbf{70}^-]$	Total
$F_1^p = g_1^p$	9	2	9	0	1	21
$F_1^n = g_1^n$	4	2	1	1	1	9

hence one may expect that at large enough Q^2 these would be constrained by perturbative QCD. In particular, at high Q^2 perturbative arguments suggest that the interaction of the photon (or W boson) should be predominantly with quarks with the same helicity as the nucleon [23,24]. Since the photon (W boson) scattering from a massless quark conserves helicity, the $\sigma_{3/2}$ cross section would be expected to be suppressed relative to the $\sigma_{1/2}$ [19]. The question then arises whether duality can exist between parton distributions at large x and resonance transitions classified according to quark *helicity* rather than spin.

In general, if the relative strengths of the $\sigma_{1/2}$ and $\sigma_{3/2}$ contributions to the cross section are weighted by $\cos^2\theta_h$ and $\sin^2\theta_h$, respectively, then from Table I the ratio of the neutron to proton F_1 structure functions can be written as

$$R^{np} = \frac{3}{7 - 5\sin^2\theta_h}, \tag{18}$$

while the proton and neutron polarization asymmetries become

$$A_1^p = \frac{7 - 9\sin^2\theta_h}{7 - 5\sin^2\theta_h}, \tag{19}$$

$$A_1^n = 1 - 2\sin^2\theta_h . \tag{20}$$

Similarly for neutrino scattering, one has

$$R^\nu = \frac{1 + \sin^2\theta_h}{5 - 4\sin^2\theta_h} \tag{21}$$

for the unpolarized structure functions, and

$$A_1^{\nu p} = \frac{1 - 3\sin^2\theta_h}{1 + \sin^2\theta_h}, \tag{22}$$

$$A_1^{\nu n} = \frac{5 - 6\sin^2\theta_h}{5 - 4\sin^2\theta_h} \tag{23}$$

for neutrino-induced polarization asymmetries. The dependence of these ratios on the mixing angle θ_h is illustrated in Figs. 2 and 3 (solid curves). For $\theta_h = \pi/4$ the SU(6) results in Eqs. (7) and (8) are once again recovered. In the phenomenologically favored region of $0 \leqslant \theta_h \leqslant \pi/4$ the predictions for A_1^p and for $A_1^{\nu n}$ are very similar to those derived on the basis of quark spin, which reflects the fact that the ratios $\Delta u/u$ are predicted to be similar in both cases. Both the $\sigma_{3/2}$ and $S_{3/2}$ suppression scenarios give rise to the same predictions for A_1^n in the $\theta \to 0$ limit, although the approach to the maximum values is faster in the case of $\sigma_{3/2}$ suppression. For the unpolarized ratios, $\sigma_{3/2}$ suppression gives rise to larger values of R^{np} and R^ν than for $S_{3/2}$ suppression. This is also evident from the modified transition strengths for F_1 and g_1 displayed in Tables IV and V for the case of $\sigma_{1/2}$ dominance at large x. Summing up the coefficients for the neutron and proton, one has in the limit $x \to 1$:

$$R^{np} = \frac{3}{7}, \quad A_1^p = 1, \quad A_1^n = 1 \ [\theta_h = 0], \tag{24}$$

for the electromagnetic ratios, and

$$R^\nu = \frac{1}{5}, \quad A_1^{\nu p} = 1, \quad A_1^{\nu n} = 1 \quad [\theta_h = 0], \tag{25}$$

for neutrino scattering.

Fitting the x dependence of the mixing angle $\theta_h(x)$ to the R^{np} data with the above $x \to 1$ constraint (Fig. 4), the resulting predictions for $A_1^{p,n}$ are shown in Figs. 5 and 6, respectively. Compared with the $S_{1/2}$ dominance scenario, the $\sigma_{1/2}$ dominance model predicts a faster approach to the asymptotic limits. The values for the ratios in Eqs. (24) and (25) correspond exactly to those calculated at the quark level on the basis of perturbative QCD counting rules [23,24]. There, the deep inelastic scattering at $x \sim 1$ requires the exchange in the initial state of two hard gluons, which preferentially enhances those configurations in the nucleon wave function in which the spectator quarks have zero helicity. The structure function at large x is then determined by components of the nucleon wave function in which the helicity of the interacting quark matches that of the nucleon. For an initial state SU(6) wave function, Eq. (9), suppression of the helicity antialigned configurations leads to the unpolarized ratio $d/u = 1/5$, and the polarization ratio $\Delta q/q = 1$ for all

TABLE V. Relative strengths of $N \to N^*$ transitions in neutrino scattering corresponding to $\sigma_{1/2}$ dominance.

SU(6) representation	$^2\mathbf{8}[\mathbf{56}^+]$	$^4\mathbf{10}[\mathbf{56}^+]$	$^2\mathbf{8}[\mathbf{70}^-]$	$^4\mathbf{8}[\mathbf{70}^-]$	$^2\mathbf{10}[\mathbf{70}^-]$	Total
$F_1^{\nu p} = g_1^{\nu p}$	0	6	0	0	3	9
$F_1^{\nu n} = g_1^{\nu n}$	25	2	16	1	1	45

quark flavors. Using the relations in the Appendix between the structure functions and the leading order quark distributions, one can verify the equivalence of the parton- and hadron-level results via quark-hadron duality.

The resulting quark-level ratios are shown in Fig. 7 for the d/u ratio, and in Figs. 8 and 9 for the $\Delta u/u$ and $\Delta d/d$ ratios, respectively. While the behavior of the $\Delta u/u$ ratio is similar in both the $S_{1/2}$ and $\sigma_{1/2}$ dominance models, the predicted $\Delta d/d$ ratio has a more rapid approach to unity for the latter case.

D. Symmetric wave function suppression

In $SU(3)\times SU(2)$ the relevant multiplets are the spin-$\frac{1}{2}$ ^{2}**8** and ^{2}**10**, and spin-$\frac{3}{2}$ ^{4}**8** and ^{4}**10**. In SU(6) the ^{2}**10** and ^{4}**8** multiplets are in the $\mathbf{70}^-$ representation, and the ^{4}**10** unambiguously in the $\mathbf{56}^+$ representation. However, the ^{2}**8** occur in both the $\mathbf{56}^+$ and $\mathbf{70}^-$. In general, for the ^{2}**8** states one can write the nucleon wave function in terms of symmetric and antisymmetric components,

$$|N\rangle = \cos\theta_w |\psi_\rho\rangle + \sin\theta_w |\psi_\lambda\rangle, \tag{26}$$

where $\psi = \varphi \otimes \chi$ is a product of the flavor (φ) and spin (χ) wave functions, and λ and ρ denote the symmetric and antisymmetric combinations, respectively [19]. In the SU(6) limit one has an equal admixture of both ρ and λ type contributions, $\theta_w = \pi/4$, and the symmetric wave function of Eq. (9) is recovered.

The SU(6) symmetry can be broken if the mixing angle $\theta_w \neq \pi/4$. In particular, if the mass difference between the nucleon and Δ is attributed to spin-dependent forces, the energy associated with the symmetric part of the wave function will be larger than that of the antisymmetric component. A suppression of the symmetric $|\psi_\lambda\rangle$ configuration at large x will then give rise to a suppressed d quark distribution relative to u, $d/u \to 0$, which in turn leads to the extreme limits for the R^{np} and R^ν ratio allowed by the quark-parton model, $R^{np} \to 1/4$ and $R^\nu \to 0$ [35]. It also leads to the proton and neutron polarization asymmetries becoming unity as $x \to 1$ [18]. At the parton level, this pattern of suppression can be realized, for instance, with a spin-dependent hyperfine interaction between quarks, $\vec{S}_i \cdot \vec{S}_j$, which modifies the spin-0 and spin-1 components of the nucleon wave function and leads to a softening of the d quark distribution relative to the u at large x (see Ref. [35] for details).

This scenario is also consistent with the absence of exotics in the t channel. This can be demonstrated by examining the pattern of suppressions in the structure function calculated, via quark-hadron duality, from the sum over resonances in the final state. In this case, the symmetric components of the states in the $\mathbf{56}^+$ and $\mathbf{70}^-$ multiplets are suppressed relative to the antisymmetric, and the modified relative transition strengths are given in Table I with $\lambda \to 0$. In particular, since transitions to the (symmetric) $S = 3/2$ or decuplet states (^{4}**8**, ^{4}**10**, and ^{2}**10**) can only proceed through the symmetric "λ" component of the ground state wave function, the "ρ" components will only excite the nucleon to ^{2}**8** states. If the λ wave function is suppressed, only transitions to ^{2}**8** states will be allowed. Summing over all channels leads to an unpolarized neutron to proton ratio in terms of the mixing angle θ_w given by

$$R^{np} = \frac{1 + 2\sin^2\theta_w}{4 - 2\sin^2\theta_w}, \tag{27}$$

with polarization asymmetries given by

$$A_1^p = \frac{6 - 7\sin^2\theta_w}{6 - 3\sin^2\theta_w}, \tag{28}$$

$$A_1^n = \frac{1 - 2\sin^2\theta_w}{1 + 2\sin^2\theta_w}. \tag{29}$$

The dependence on θ_w is shown in Fig. 2. In the limit of ρ dominance at $x \to 1$, one recovers the ratios

$$R^{np} = \frac{1}{4}, \quad A_1^p = 1, \quad A_1^n = 1 \quad [\theta_w = 0]. \tag{30}$$

Fitting θ_w to the x dependence of R^{np} in Fig. 4 with the above constraints (dot-dashed), the resulting x dependence of the polarization asymmetries A_1^p and A_1^n are shown in Figs. 5 and 6 (dot-dashed). The approach to the asymptotic values for the polarization asymmetries is less rapid than for the $\sigma_{1/2}$ or $S_{1/2}$ dominance scenarios.

Similarly, for neutrino scattering, one has

$$R^\nu = \frac{2\sin^2\theta_w}{3 - 2\sin^2\theta_w}, \tag{31}$$

and

$$A_1^{\nu p} = -\frac{1}{3}, \tag{32}$$

$$A_1^{\nu n} = \frac{9 - 10\sin^2\theta_w}{9 - 6\sin^2\theta_w}, \tag{33}$$

for neutrino-induced polarization asymmetries. Note that the neutrino-proton polarization asymmetry remains negative, as in SU(6), and is independent of the mixing angle. The dependence on θ_w of the ratios is illustrated in Figs. 2 and 3 (dot-dashed curves), where in the limit $\theta_w \to 0$ ($x \to 1$) one has

$$R^\nu = 0, \quad A_1^{\nu p} = -\frac{1}{3}, \quad A_1^{\nu n} = 1 \quad [\theta_w = 0]. \tag{34}$$

The ratios of the associated quark densities are given in Figs. 7–9 for d/u, $\Delta u/u$, and $\Delta d/d$, respectively. Because the neutron asymmetry $A_1^{\nu n}$ is negative, the predicted $\Delta d/d$ ratio has qualitatively different behavior in the λ suppression scenario than in the other two SU(6) broken models. It would clearly be of considerable interest to test the behavior of $\Delta d/d$ experimentally, for instance in semi-inclusive deep inelastic scattering by tagging pions.

IV. IMPLICATIONS FOR LOW-LYING RESONANCES

If the suppression of specific spin-flavor correlations, as required to fit the $x \to 1$ behavior of structure functions, is a property of spin-dependent interquark forces, then they should affect specific resonances that share these properties. In this section we identify some examples and propose measurements that can test the veracity of the various scenarios discussed in Sec. III.

A. Suppression of $^4\mathbf{10}$ states

If the suppression of the $P_{33}(1232)$ Δ isobar at large Q^2 is characteristic of $^4\mathbf{10}$ and $^4\mathbf{8}$ states, then a careful study of electroproduction of the $L=2$ $\mathbf{56}^+$ states $P_{31}(1930)$, $P_{33}(1920)$, $F_{35}(1905)$, and $F_{37}(1950)$ may reveal $S_{3/2}$ suppression as the appropriate physical mechanism responsible for symmetry breaking in structure functions at large x. Transitions to each of these states, in the absence of configuration mixing, should die relatively faster with Q^2 than for the $^2\mathbf{8}$ and $^2\mathbf{10}$ resonances. This should be particularly so for the $F_{37}(1950)$, where mixing should be minimal, although one must ensure to have gone past the high angular momentum threshold that may cause the form factors for high spin states to remain large in the small Q^2 region.

A possible way to normalize the production, and cancel out such threshold enhancements, will be to compare the relative strengths of these $^4\mathbf{10}$ and their partner $^2\mathbf{8}[\mathbf{56}^+]$ states. Thus measurement of the Q^2 dependence of ratios such as

$$F_{35}(1905)/F_{15}(1680); P_{33}(1920)/P_{13}(1720)$$

would be crucial in testing this scenario.

B. Suppression of $^4\mathbf{8}$ states

In general, mixing is expected between the $^4\mathbf{8}$ and $^2\mathbf{8}$ states with the same J^P. For example, the physical $S_{11}(1550)$ and $S_{11}(1650)$ states are superpositions of $^2\mathbf{8}$ and $^4\mathbf{8}$ components:

$$S^a_{11}(1535) = \cos\theta |^2 8\rangle + \sin\theta |^4 8\rangle, \tag{35}$$

$$S^b_{11}(1650) = \sin\theta |^2 8\rangle - \cos\theta |^4 8\rangle, \tag{36}$$

and similarly for the $D_{13}(1520)$ and $D_{13}(1700)$ states. From protons one then expects

$$\frac{\sigma(\gamma^* p \to S^a_{11})}{\sigma(\gamma^* p \to S^b_{11})} \sim \cot^2\theta, \tag{37}$$

which will be true for all Q^2, as the $^4\mathbf{8}$ component is not excited. From neutron targets, however, both components are excited at low Q^2, whereas the $^4\mathbf{8}$ is suppressed at large Q^2. Hence at small Q^2 one has

$$\frac{\sigma(\gamma^* n \to S^a_{11})}{\sigma(\gamma^* n \to S^b_{11})} \sim f(\theta), \tag{38}$$

where $f(\theta)$ is a function of the mixing angle and of the relative strengths of the $^2\mathbf{8}$ and $^4\mathbf{8}$ photocouplings. However, at large Q^2 only the $^2\mathbf{8}$ is predicted to survive (thus in effect the Moorhouse selection rule [36] will hold for neutrons too when $Q^2 \to \infty$), in which case

$$\left.\frac{\sigma(\gamma^* n \to S^a_{11})}{\sigma(\gamma^* n \to S^b_{11})}\right|_{Q^2\to\infty} \to \cot^2\theta \equiv \left.\frac{\sigma(\gamma^* p \to S^a_{11})}{\sigma(\gamma^* p \to S^b_{11})}\right|_{\text{all } Q^2}. \tag{39}$$

As this behavior is predicted to be common for p and n targets, it should therefore hold true for the deuteron. The $D_{15}(1690)$ is a pure $^4\mathbf{8}$ state and so provides a clean test of the fast Q^2 suppression in electroproduction from neutron targets.

C. Suppression of $\sigma_{3/2}$

The suppression of helicity-$\frac{3}{2}$ contributions allows transitions to the Δ to survive, as well as excitations to the $^4\mathbf{8}$ states from the neutron (those from the proton vanish because of the Moorhouse selection rule [36]). At $Q^2=0$, the Δ excitation is pure $M1$, which equates with $\sigma_{3/2}=3\sigma_{1/2}$, and leads to the polarization asymmetry $A_1^N=-1/2$. At large Q^2 the survival of the Δ, in the $\sigma_{3/2}$ channel, corresponds to the $E2$ excitation becoming comparable to the $M1$.

Electroproduction of the S_{11}, D_{13}, and D_{15} resonances from neutrons will change from $A_1^N=-1/2$ to $A_1^N=1$. This should remain true for the D_{15}, but can be obscured by mixing with $^2\mathbf{8}$ for the S_{11} and D_{13}. Configuration mixing between the $^2\mathbf{8}$ and $^4\mathbf{8}$ states (with mixing angle $\sim 30°$) does allow a relatively strong transition to the $S_{11}(1650)$. Data from CLAS at Jefferson Lab [17] suggest that, within the single quark transition model [37], the strength of the $S_{11}(1650)$ transition is about half of that to the $S_{11}(1535)$. The mixing angle between the $^4\mathbf{8}$ and $^2\mathbf{8}$ states with $J^P=\frac{3}{2}^-$ is much smaller ($\sim 6°$), so that transitions to the $D_{13}(1700)$ will be weakly excited from the proton. The strengths for the other $^4\mathbf{8}$ states are known only at $Q^2=0$, so that data on these transition form factors at $Q^2 \sim 1$–2 GeV^2 would be valuable in establishing the extent of any suppression.

D. Suppression of ψ_λ wave function

The consequences for N^*s in this scenario are quite extensive. Namely, transitions to $^4\mathbf{10}$, $^4\mathbf{8}$, and $^2\mathbf{10}$ states are all suppressed, and only transitions to $^2\mathbf{8}$ are allowed. While the transitions for the proton to $^2\mathbf{8}$ are unchanged compared with the SU(6) case, for neutron the elastic transition is reduced by $\sim 50\%$, and the transition to the $\mathbf{70}^-$ enhanced by $\sim 50\%$.

Another prediction of λ wave function suppression is identical production rates in both the $\mathbf{56}^+$ and $\mathbf{70}^-$ channels, for electron and neutrino scattering. For the latter, essentially no empirical information exists, however, neutrino structure functions in the resonance region may be accessible in the future at a high-intensity neutrino beam facility [15]. In particular, since neutrinos can excite protons *only* to decuplet

states, this may provide a valuable test of the λ-suppression mechanism, and of the isospin dependence of the $N \to N^*$ transitions.

V. CONCLUSION

In this analysis we have performed a first detailed study of the conditions under which SU(6) symmetry breaking in the quark model can yield consistent results for structure function ratios in the context of quark-hadron duality. Several self-consistent SU(6) breaking scenarios have been identified, involving the suppression of transitions to states in the lowest even and odd parity multiplets with quark spin $S=3/2$, to states with helicity $\frac{3}{2}$, and to states which couple only through symmetric components of the wave function, ψ_λ.

The implications of the various symmetry breaking scenarios on the x dependence of structure function ratios have been quantified, which can be tested in future experimental studies. In particular, fitting to the available data on the unpolarized neutron to proton ratio R^{np} allows one to make predictions for the large x behavior of polarization asymmetries A_1^N. Experiments proposed at an energy-upgraded Jefferson Lab should enable the R^{np} ratio to be reliably determined up to $x \sim 0.85$ [30,31]. For the polarization asymmetries there is existing evidence that $A_1^p > 5/9$ at $x \gtrsim 0.6$, and recent data on A_1^n from Hall A at Jefferson Lab [38,39] give the first hint of a rise above zero at $x \sim 0.6$. High-precision data on A_1^p or A_1^n at large x would help constrain also the unpolarized n/p ratio, and allow a simultaneous test of the duality relations.

Measurement of the neutrino structure function ratios, on the other hand, is more challenging due to the low rates at large x, and the need for large volume (typically iron) targets, which is particularly problematic for the spin-dependent observables. The prospect of high-intensity neutrino beams at Fermilab to measure structure functions in the resonance region [15] offers a valuable complement to the study of duality and resonance transitions. A parallel avenue towards determining the spin-flavor asymmetries such as $\Delta u/u$ and $\Delta d/d$, which is particularly sensitive to different SU(6) breaking assumptions, could be provided through a program of semi-inclusive scattering tagging fast pions in the current fragmentation region.

A quantitative description of transition form factors in the quark model at moderate Q^2 must involve both longitudinal and transverse response, electric, and magnetic couplings, as well as hyperfine interactions which explicitly break SU(6) symmetry. On the other hand, most of these complications do not affect the main elements of duality, and can obfuscate the basic principles which drive the quark-hadron transition. For reasons of clarity, in the present analysis we have considered only magnetic transitions, which are expected to dominate at high Q^2. This assumption leads, for instance, to the electromagnetic neutron to proton ratio $R^{np}=4/9$ for the case of elastic scattering, which is equal to the squared ratio of the neutron to proton magnetic moments in SU(6) [2,40]. Electric transitions would give a ratio $R^{np}=0$. Electric couplings will also modify the coefficients in Tables I and II for the other transitions [9]. Although electric couplings will play a role at low Q^2, for the behavior of structure functions at large x one expects magnetic couplings to dominate the transition form factors at high Q^2.

In future we shall extend this work to the longitudinal structure function, which will necessitate inclusion of electric couplings. Questions about the role of higher excitations, such as in the $N=2$, $L=2$ band, will also be important to elucidate in more refined analyses. There are a number of states with mass $W \lesssim 1.8$ GeV which belong to higher multiplets, such as the $F_{15}(1680)$, which is believed to play an important role in the third resonance region. In addition, it will be interesting to ascertain the role played by the $P_{11}(1440)$ Roper resonance in duality, which may shed some light on the long-standing question about its internal structure [41].

ACKNOWLEDGMENTS

We would like to thank V. D. Burkert for helpful discussions. This work was supported by the U.S. Department of Energy, Contract No. DE-AC05-84ER40150, under which the Southeastern Universities Research Association (SURA) operates the Thomas Jefferson National Accelerator Facility (Jefferson Lab), and by grants from the Particle Physics and Astronomy Research Council, and the EU program ''Eurudice'' HPRN-CT-2002-0031.

APPENDIX: PARTON MODEL AND DUALITY RELATIONS

Here we summarize the quark-parton model relations between electromagnetic and neutrino structure functions and leading order parton distributions. The spin-averaged and spin-dependent F_1 and g_1 structure functions are expressed in terms of a sum and difference of helicity cross sections,

$$F_1 \sim \sigma_{1/2} + \sigma_{3/2}, \tag{A1}$$

$$g_1 \sim \sigma_{1/2} - \sigma_{3/2}, \tag{A2}$$

where $\sigma_{1/2(3/2)}$ is the cross section corresponding to total boson-nucleon helicity 1/2 (3/2).

In the parton model the structure functions for charged lepton scattering can be expressed (at leading order) in terms of quark distribution functions,

$$F_1(x) = \frac{1}{2} \sum_q e_q^2 q(x), \tag{A3}$$

$$g_1(x) = \frac{1}{2} \sum_q e_q^2 \Delta q(x), \tag{A4}$$

where $q = q^\uparrow + q^\downarrow$ and $\Delta q = q^\uparrow - q^\downarrow$. Inverting these, one can similarly extract leading order quark distributions from the measured structure functions. For instance, the d/u quark distribution ratio can be determined from

$$\frac{d}{u}=\frac{4R^{np}-1}{4-R^{np}}, \tag{A5}$$

where $R^{np}=F_1^n/F_1^p$, while the spin-dependent flavor ratios for the u and d quarks are obtained from the polarization asymmetries and the d/u ratio in Eq. (A5) [39],

$$\frac{\Delta u}{u}=\frac{4}{15}A_1^p\left(4+\frac{d}{u}\right)-\frac{1}{15}A_1^n\left(1+4\frac{d}{u}\right), \tag{A6}$$

$$\frac{\Delta d}{d}=-\frac{1}{15}A_1^p\left(1+4\frac{u}{d}\right)+\frac{4}{15}A_1^n\left(4+\frac{u}{d}\right), \tag{A7}$$

where

$$A_1^p=\frac{4\Delta u+\Delta d}{4u+d}, \tag{A8}$$

$$A_1^n=\frac{\Delta u+4\Delta d}{u+4d}. \tag{A9}$$

Note that if $A_1^p=A_1^n\equiv A_1^N$, then $\Delta u/u=\Delta d/d=A_1^N$, independent of the value of d/u.

For neutrino scattering one has

$$F_1^\nu(x)=\sum_q g_q^2 q(x), \tag{A10}$$

$$g_1^\nu(x)=\sum_q g_q^2 \Delta q(x), \tag{A11}$$

where for protons $g_q^2=1$ for $q=d,\bar{u},\ldots$ and 0 for $q=u,\bar{d},\ldots$, and vice versa for neutrons. At large x therefore $F_1^{\nu p}$, $g_1^{\nu p}$ directly probe the d quark distributions, while $F_1^{\nu n}$, $g_1^{\nu n}$ probe the u quark. In terms of the neutrino structure functions, the unpolarized ratio $R^\nu=F_1^{\nu p}/F_1^{\nu n}$ is therefore given by

$$R^\nu=\frac{d}{u}, \tag{A12}$$

while the polarization asymmetries $A_1^{\nu N}=g_1^{\nu N}/F_1^{\nu N}$ become

$$A_1^{\nu p}=\frac{\Delta d}{d}, \tag{A13}$$

$$A_1^{\nu n}=\frac{\Delta u}{u}. \tag{A14}$$

[1] I. Niculescu *et al.*, Phys. Rev. Lett. **85**, 1182 (2000); **85**, 1186 (2000).

[2] E.D. Bloom and F.J. Gilman, Phys. Rev. Lett. **25**, 1140 (1970); Phys. Rev. D **4**, 2901 (1971).

[3] A. De Rújula, H. Georgi, and H.D. Politzer, Ann. Phys. (N.Y.) **103**, 315 (1977).

[4] M. E. Christy, in *Proceedings of the 9th International Conference on the Structure of Baryons, Jefferson Lab, 2002*, edited by C. Carlson and B. Mecking (World Scientific, Sinapore, 2003); M. E. Christy, R. Ent, C. Keppel *et al.* (unpublished).

[5] V.D. Burkert, in *Mesons and Light Nuclei*, edited by Jirí Adam, Petr Bydzovský, and Jirí Mares, AIP Conf. Proc. **603** (AIP, Melville, NY, 2001), p. 3; T. Forest, in *Proceedings of the 9th International Conference on the Stucture of Baryons, Jefferson Lab, 2002*, edited by C. Carlson and B. Mecking (World Scientific, Singapore, 2003).

[6] N. Liyanage, Contact person, Jefferson Lab Experiment E01-012.

[7] F.E. Close, F.J. Gilman, and I. Karliner, Phys. Rev. D **6**, 2533 (1972).

[8] F.E. Close and F.J. Gilman, Phys. Rev. D **7**, 2258 (1972).

[9] F.E. Close, H. Osborn, and A.M. Thomson, Nucl. Phys. **B77**, 281 (1974).

[10] J. Kuti and V.F. Weisskopf, Phys. Rev. D **4**, 3418 (1971).

[11] F.E. Close and F.J. Gilman, Phys. Lett. **38B**, 541 (1972).

[12] F.E. Close and N. Isgur, Phys. Lett. B **509**, 81 (2001).

[13] N. Isgur, S. Jeschonnek, W. Melnitchouk, and J.W. Van Orden, Phys. Rev. D **64**, 054005 (2001).

[14] M.W. Paris and V.R. Pandharipande, Phys. Lett. B **514**, 361 (2001); Phys. Rev. C **65**, 035203 (2002); S. Jeschonnek and J.W. Van Orden, Phys. Rev. D **65**, 094038 (2002); F.E. Close and Q. Zhao, *ibid.* **66**, 054001 (2002).

[15] J. Morfin *et al.*, *Expression of Interest to Perform a High-Statistics Neutrino Scattering Experiment using a Fine-grained Detector in the NuMI Beam*, presented to FNAL PAC, November 2002.

[16] L.A. Copley, G. Karl, and E. Obryk, Phys. Rev. D **4**, 2844 (1971); Nucl. Phys. **B13**, 303 (1969).

[17] V.D. Burkert, R. De Vita, M. Battaglieri, M. Ripani, and V. Mokeev, Phys. Rev. C **67**, 035204 (2003).

[18] F.E. Close, Nucl. Phys. **B80**, 269 (1974).

[19] F. E. Close, *Introduction to Quarks and Partons* (Academic, London, 1979).

[20] L.W. Whitlow *et al.*, Phys. Lett. B **282**, 475 (1992).

[21] J. Gomez *et al.*, Phys. Rev. D **49**, 4348 (1994).

[22] W. Melnitchouk and A.W. Thomas, Phys. Lett. B **377**, 11 (1996).

[23] G.R. Farrar and D.R. Jackson, Phys. Rev. Lett. **35**, 1416 (1975).

[24] J.F. Gunion, P. Nason, and R. Blankenbecler, Phys. Rev. D **29**, 2491 (1984).

[25] P. Stoler, Phys. Rev. D **44**, 73 (1991).

[26] C.E. Carlson and N.C. Mukhopadhyay, Phys. Rev. D **47**, 1737 (1993); Phys. Rev. Lett. **81**, 2646 (1998).

[27] A. De Rújula, H. Georgi, and S.L. Glashow, Phys. Rev. D **12**, 147 (1975).

[28] L.L. Frankfurt and M.I. Strikman, Phys. Rep. **76**, 215 (1981).

[29] W. Melnitchouk and A. W. Thomas, in *Testing QCD Through Spin Observables in Nuclear Targets* (World Scientific, Singapore, 2003), nucl-th/0207056.

[30] I.R. Afnan, F. Bissey, J. Gomez, A.T. Katramatou, W. Melnitchouk, G.G. Petratos, and A.W. Thomas, Phys. Lett. B **493**, 36 (2000); E. Pace, G. Salme, S. Scopetta, and A. Kievsky, Phys. Rev. C **64**, 055203 (2001).

[31] W. Melnitchouk, M. Sargsian, and M.I. Strikman, Z. Phys. A **359**, 99 (1997); S. Kuhn, Contact person, Jefferson Lab experiment E03-012.

[32] P.L. Anthony *et al.*, Phys. Rev. D **54**, 6620 (1996); K. Abe *et al.*, Phys. Rev. Lett. **79**, 26 (1997); K. Abe *et al.*, Phys. Rev. D **58**, 112003 (1998).

[33] D. Adams *et al.*, Phys. Lett. B **357**, 248 (1995); B. Adeva *et al.*, Phys. Rev. D **60**, 072004 (1999).

[34] K. Ackerstaff *et al.*, Phys. Lett. B **404**, 383 (1997); A. Airapetian *et al.*, HERMES Collaboration, Phys. Rev. Lett. **90**, 092002 (2003).

[35] R. P. Feynman, *Photon Hadron Interactions* (Benjamin, Reading, Massachusetts, 1972); F.E. Close, Phys. Lett. **43B**, 422 (1973); R. Carlitz, *ibid.* **58B**, 345 (1975); R.D. Carlitz and J. Kaur, Phys. Rev. Lett. **38**, 673 (1977); F.E. Close and A.W. Thomas, Phys. Lett. B **212**, 227 (1988); N. Isgur, Phys. Rev. D **59**, 034013 (1999).

[36] R.G. Moorhouse, Phys. Rev. Lett. **16**, 772 (1966).

[37] W.N. Cottingham and I.H. Dunbar, Z. Phys. C **2**, 41 (1979); A.J.G. Hey and J. Weyers, Phys. Lett. **48B**, 69 (1974).

[38] Z.-E. Meziani, Contact person, Jefferson Lab Experiment E99-117; Z.-E. Meziani, hep-ex/0302020.

[39] X. Zheng, Ph.D. thesis, MIT, 2002; X. Zheng *et al.*, nucl-ex/0308011.

[40] W. Melnitchouk, Phys. Rev. Lett. **86**, 35 (2001).

[41] W. Melnitchouk *et al.*, CSSM Lattice Collaboration, Phys. Rev. D **67**, 114506 (2003); Nucl. Phys. B (Proc. Suppl.) **109A**, 96 (2002).